JOURNAL OF MATERIALS SCIENCE 35 (2000) 4319–4324

Influence of temperature on the fracture of a W-Ni-Fe alloy

R. G. O'DONNELL
CSIRO Manufacturing Science and Technology, Private Bag 33, Clayton Sth MDC 3168, Australia
E-mail: odonnell@cmst.csiro.au

R. L. WOODWARD†
DSTO AMRL, PO Box 50, Ascot Vale 3032 Victoria, Australia

A 95wt%W 3.5wt%Ni 1.5wt%Fe alloy is strained to failure in uniaxial tension at temperatures in the range −100°C to 300°C. The fracture surfaces of the tensile specimens are examined and the contributions from the fracture mechanisms: tungsten-tungsten intergranular decohesion, tungsten-binder interface decohesion, binder rupture and tungsten cleavage, are identified as a function of temperature. The observed variations are explained in terms of the flow stress temperature dependence of the two phases within the alloy. The results are consistent with a changing mode of specimen rupture from one of a localized cascade of nucleation events at low temperatures to one of crack propagation through linking of cracks within the necked region of the specimens deformed at higher temperatures.

1. Introduction

The fabrication of W-Ni-Fe alloys by liquid phase sintering has continued to receive attention since their development in the 1940's [1]. Several researchers have investigated the effects of heat treatment, cold work, microstructure and compositional variations on toughness and other mechanical properties [2–7]. The refinement of sintering conditions [8–12], the role of precipitation within these alloys [13, 14] and the variation in their mode of fracture with microstructure [2–6, 10, 11] have also received attention.

The liquid phase sintering of W-Ni-Fe alloys produces a microstructure comprising a semicontiguous network of spheroidal BCC tungsten grains (containing a small amount of nickel and iron in solution) in a FCC Ni-Fe-W binder (matrix). The semicontiguous nature of these alloys contributes to the available fracture mechanisms. Failure can occur through a combination of four principal mechanisms [2, 4, 6], namely: (i) decohesion between adjacent tungsten grains (W-W), (ii) decohesion between the tungsten grains and the binder (W-B), (iii) ductile rupture of the binder (B) and (iv) transgranular cleavage of the tungsten grains (W cleavage).

Ekbom [3] has shown that during tensile straining at room temperature the initial strain in these composite tungsten/binder alloys is accommodated within the binder phase which strain hardens to approach the strength of the tungsten grains during the first 3% deformation. Beyond 5% deformation, the binder and tungsten grains are shown to deform equally. The ability of these two phases to apportion the load between them will determine their ultimate strength, ductility and mode of fracture. The mechanical properties of these alloys depend on the strength and ductility of both the tungsten and the binder phase and on the cohesive strength of the W-W and W-binder interfaces.

Among the four fracture mechanisms, numerous authors have identified the decohesion of the tungsten grains as the fracture mechanism requiring the least energy [2, 4–6, 10, 11, 13, 15, 16]. These decohesion sites act as cracks within the deforming body and as notches when these occur at the sample surface [5, 10, 12]. An increase in contiguity between tungsten grains, which is generally associated with an increased tungsten grain size (typically achieved through either increased sinter temperature, duration, or higher tungsten content [2, 12]), leads to an increase in the size of the W-W interface areas and hence in the size of the 'cracks' within these alloys. An increase in the occurrence of the W-W decohesion mechanism has been determined by several authors to reduce both strength and ductility in these alloys [2, 3, 6, 11].

It is common to observe sites of W-W decohesion within these materials at an early stage of deformation [3] or after fracture has occurred, in regions away from the fracture surface in sectioned tensile specimens [2, 6]. Calculations indicate that such cracks, associated with W-W decohesion, are subcritical [17] suggesting rupture in these materials relies on a mechanism which enables these cracks to grow and/or link up [17].

† Deceased.

On the other hand, among the remaining three fracture mechanisms, cleavage of the tungsten grains is considered to require the greatest energy input [11]. The strength of the W-binder cohesion can be dependent on the segregation of impurities to the interface. This segregation is detrimental to cohesive strength and is increased by slow cooling rates from post sintering anneals [4, 5]. As a result, alloys which undergo slow cooling conditions typically demonstrate a higher proportion of W-binder decohesion. The occurrence of binder rupture, on the other hand, is dependent on the relative strength of this phase and whether it is energetically favoured as compared to the other three.

Earlier work by the present authors [2] has identified the contribution of these four fracture mechanisms to the room temperature failure of several W-Ni-Fe alloys. The alloy which is the subject of the present investigation, namely W 3.5wt%Ni 1.5wt%Fe, was found to have a high tensile fracture strain combined with a high ultimate tensile strength and has Defence application as a kinetic energy penetrator [8]. The mechanism of fracture within this alloy at room temperature can be summarised as follows: beyond a critical load, W-W intergranular decohesion is initiated in those weaker W-W contact regions which are oriented approximately normal to the tensile axis; continued loading of the surrounding matrix phase then leads to an increase in the number of W-W separation cracks until load shedding and a cascade of crack nucleation events throughout a narrow zone in the cross section, involving all four fracture mechanisms, results in specimen rupture.

The present work seeks to extend these observations to the failure of the W 3.5%Ni 1.5%Fe alloy at temperatures between -100°C and $+300^{\circ}$C.

2. Experimental

The liquid phase sintered tungsten alloy, with composition 95wt%W 3.5wt%Ni 1.5wt%Fe, was supplied by the Australian Hard Materials division of Sandvik Pty Ltd. and has been fully characterised in a previous publication [2]. The grain size was approximately 34 μm.

Tensile tests were conducted with the aid of a Riehle tensile testing machine using a 50 kN load cell, an initial strain rate of 1.14×10^{-3} s^{-1} and an LVDT to electronically monitor cross-head displacement. All tests were repeated at least once.

Two sizes of dumbbell shaped specimens were used for the tensile tests. Specimens conformed to AS1391-1991 with either a gage length of 35.80 mm and gage diameter 7.15 mm or a gage length of 20.0 mm and gage diameter 4.0 mm.

Test temperatures below room temperature were achieved using an alcohol bath cooled with either ice, solid CO_2 or liquid nitrogen with the test conducted below the cross-head to enable immersion in the bath. Warm temperatures were achieved with the aid of an electrically heated split furnace mounted between the cross-heads.

The load was recorded directly from the Riehle load cell and the failure strain measured by repositioning the two fractured sections and recording the separation between previously inscribed gage length marks.

An examination of fracture surfaces of tensile test specimens in the scanning electron microscope (SEM) allowed the contributions of W-W, W-B, B and W fractures to be assessed. The measurements were made by superimposing a grid (1 mm graph paper) onto 2 or 3 representative micrographs from each fracture surface.

3. Results

The ultimate tensile strength (UTS) and failure strain for tests at each temperature are plotted in Fig. 1. An arrow indicates the temperatures above which straining produced a neck in the sample.

This alloy demonstrates a continuous decrease in UTS with increasing temperature while the failure strain approaches a maximum of approximately 30% between 50 and 100°C. This trend is consistent with data collected from tensile tests on 10 different alloys and from torsion tests on an identical alloy over a similar range of temperatures during previous investigations [12, 18]. All these data are consistent with this alloy undergoing a ductile to brittle transition (DBT) at about room temperature.

Typical fracture surfaces from samples loaded at -50°C and 150°C are presented in Fig. 2a and b respectively. Fig. 2a is an SEM image which uses backscattered electrons to improve elemental contrast between the phase rich in tungsten [high atomic number, appearing white in Fig. 2a] and the Ni/Fe phase [lower atomic number, darker areas of contrast in Fig. 2a]. Each of the four principal fracture mechanisms described in the previous section are evident within Fig. 2a. The smooth, rounded shapes on the surface of the tungsten phase, such as A in Fig. 2a are the sites of W-W intergranular decohesion. There is no evidence of any binder phase within these rounded contact sites suggesting that the binder phase is excluded from these regions during spheroid growth in sintering. The remaining smooth regions on the surface of the tungsten rich phase [such as B in Fig. 2a] are indicative of the W-B decohesion mechanism.

These latter regions tend to surround the sites of W-W intergranular decohesion. The third fracture mode, which is also evident in the tungsten rich phase, is the transgranular fracture of the tungsten grains themselves

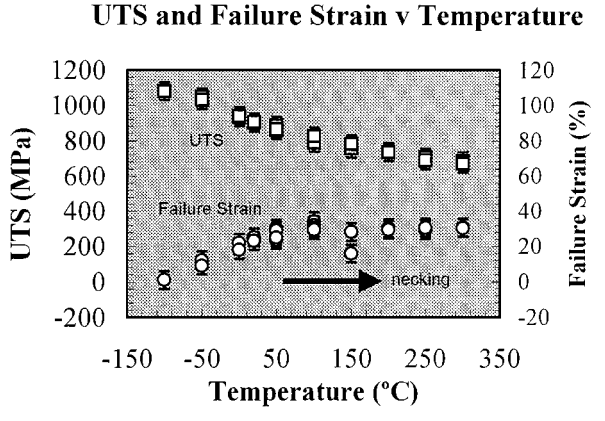

Figure 1 Variation of UTS and Failure strain with Temperature. The arrow indicates the temperature range where necking occurs during tensile testing.

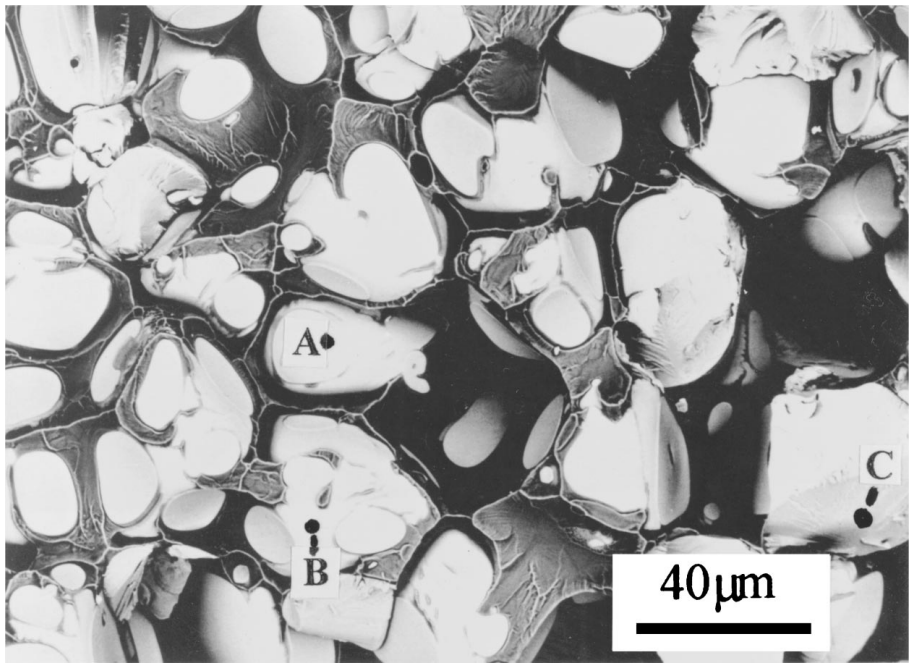

(a)

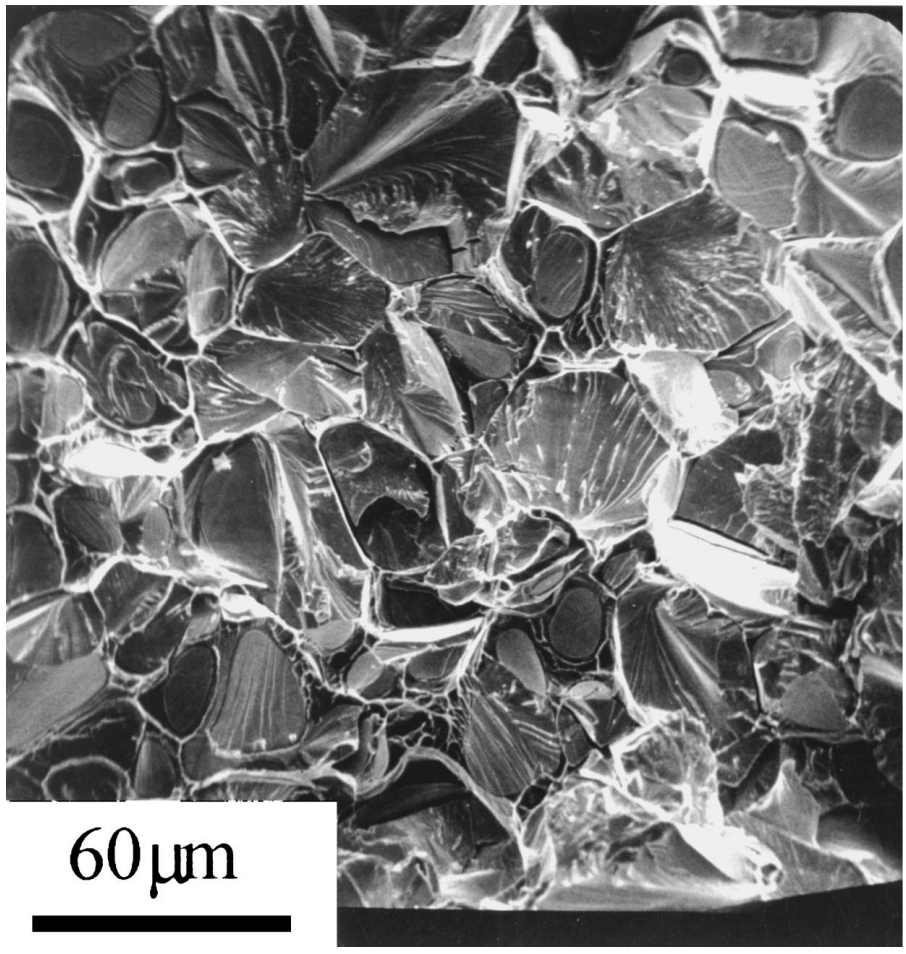

(b)

Figure 2 Scanning electron micrographs of fracture surface from specimens tested at (a) −50°C and (b) 150°C. The detection of backscattered electrons is used in (a) to highlight elemental contrast.

[C in Fig. 2a]. The fourth fracture mechanism evident in Fig. 2a is the rupture of the darker binder phase.

Fig. 2b is a secondary electron image of the fracture surface of a sample strained to failure at 150°C. Apart from the reduced elemental contrast, this surface appears significantly different to that in Fig. 2a. Whilst some W-W decohesion is evident in this figure, the majority of the fracture surface is comprised of W cleavage. The contribution of each of the fracture mechanisms to the final failure was noted to depend

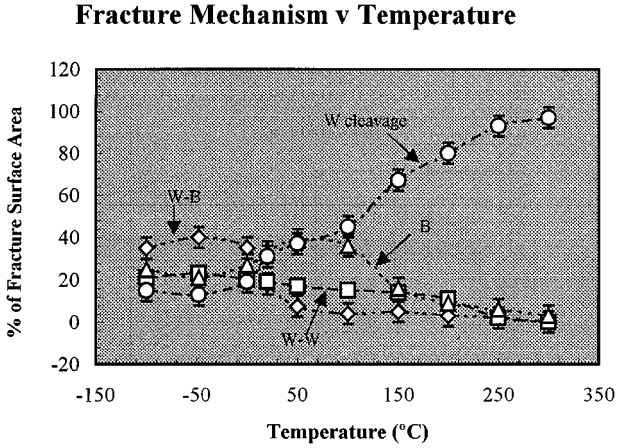

Figure 3 Contribution to the fracture surface from the different fracture mechanisms as a function of temperature.

TABLE I Contribution to the fracture surface from individual fracture mechanisms

Test Temperature (°C)	W-B (%)	W-W (%)	Binder Rupture (%)	W cleavage (%)
−100	35	21	25	15
−50	40	23	21	13
0	35	20	27	19
20	18	19	33	31
50	7.5	17	39	37
100	4.0	15	36	45
150	5.0	14	16	67
200	3.0	11	9	80
250	2.0	2	6	93
300	0.0	0	3	97

on test temperature and this variation is summarised in Fig. 3.

It is clear from Fig. 3 that the contribution of W-W decohesion to the fracture surface decreases slowly with increasing temperature up to approximately 200°C where it decreases more rapidly. The occurrence of W-B decohesion is greatest at lower temperatures reducing to less than 5% of the total fracture area at 100°C. Binder rupture increases from approximately 20% below 0°C to approximately 40% of the total fracture surface area between 50 and 100°C. The contribution from binder rupture then falls off rapidly above 100°C. The prevalence of W cleavage increases with temperature above approximately 0°C and becomes the dominant mechanism above approximately 100°C. By 250°C, W cleavage covers more than 90% of the total fracture surface area.

4. Discussion

In order to better understand the variation in fracture behaviour with temperature, the conditions which favour each of the four fracture modes, W-W interfacial decohesion, W-B interfacial decohesion, W cleavage and binder phase rupture, need to be identified and their interactions considered in the light of the temperature dependence of the flow properties of each phase.

Room temperature mechanical testing of binder phase material alone [19] shows the binder to have about one third the flow stress of the 95% W alloy itself and to withstand the yield stress of the 95% W alloy would undergo about 30% plastic strain. Microhardness tests on the binder phase and on the tungsten grains in the 95%W alloy suggest that mutual confinement reduces the strength differential between these two phases [20] resulting in less strain in the binder phase being required before a general plastic state is attained as suggested by Ekbom [3]. The strength differential between these phases will also vary with temperature as the flow stress of the tungsten phase is more sensitive to temperature than is that of the binder [4].

The strain differential which develops between binder and tungsten grains whilst the body undergoes initial deformation generates a high component of shear at the W-binder interface. The toughness of this interface, the magnitude of this shear and the proximity to other defects such as W-W decohesion sites will determine whether fracture will initiate at this site. Ostalaza Zamora *et al*. [6] have shown the cohesive strength of the W-binder interface plays a significant role in the distribution of loads within the deforming body. These authors examined the role of the ligaments of binder phase that bridge the W-W decohesion sites, in the fracture of these alloys. They concluded that for alloys which demonstrate poor W-binder cohesion, the decohesion of unfavourably oriented W-binder interfaces, further transfers the stress to the ductile binder ligaments which then tend to fail through ductile shear. This produces an overall fracture surface which is a mixture of W-W decohesion, W-binder decohesion and binder rupture with only a small minority of W cleavage. Similar fracture surface characteristics have been noted for less ductile alloys by several investigators [2, 4, 11]. Alloys which demonstrate strong W-binder cohesion typically have higher ductility as the ligaments of binder phase are able to effectively transfer load to the tungsten grains. Failure in these materials is typically through binder rupture and cleavage of the tungsten grains [2, 5, 6].

The present alloy demonstrates good ductility and a fracture surface which comprises about 30% W-cleavage at room temperature. This is consistent with an alloy which has strong W-binder cohesion and which therefore does not suffer from significant impurity segregation to these interfaces.

The increased presence of W-B failure below room temperature during the present tests, as seen in Fig. 3, is consistent with a tungsten phase which is much stiffer than the surrounding binder at these temperatures and the consequent generation of excessive shear at this interface during deformation. The rapid decrease in the contribution from W-B fracture at temperatures greater than 0°C is also consistent with a tungsten phase which undergoes gradual preferred softening relative to the less temperature sensitive binder phase and therefore reduces the strain differential across this interface during deformation above 0°C. The increase in uniform plastic strain (refer to Fig. 1) and in W cleavage fracture above 0°C supports this interpretation.

The contribution from binder phase rupture to the fracture surface in this alloy follows the increase in

contribution from W cleavage up to approximately 100°C and then drops off to a much smaller contribution above this. As test temperatures approach 100°C, the relative increase in strength of the W-B mechanism shifts the preferred mode of fracture to the two similarly weak mechanisms of binder rupture and W cleavage, thus accounting for the increased operation of both these mechanisms. At higher temperatures still, where the tungsten phase softens further, W cleavage is expected to be favoured over binder rupture and thus account for the complete dominance of the W cleavage mechanism at high temperatures seen in Fig. 3. However, Rabin and German [10] point out that when there is no preferred crack path, the fracture surface should be representative of the microstructure. On a phase volume fraction basis this would tend to suggest 84% cleavage and 16% binder phase rupture in the present alloy (where W-W and W-B are not included in this simple analysis). The high contribution from W cleavage at high temperatures may then simply be due to a nonpreference for a fracture path although a preference for cleavage of the softer tungsten phase may still persist.

Fig. 3 demonstrates that the proportion of the total fracture surface area occupied by W-W decohesion sites reduces only slightly from −100°C to 200°C. This is similar to the results of German *et al.* [4] who determine the proportion of W-W decohesion to be constant for Charpy impact tests on a nominally identical alloy at temperatures of −100°C, 22°C and 300°C. The presence of a similar proportion of W-W decohesion in all fracture surfaces up to 200°C is consistent with this being the lowest energy mechanism which operates at an early stage of fracture.

A relatively small number of W-W intergranular decohesion sites have been observed away from the surface of rupture in sectioned specimens of nominally identical composition deformed at room temperature [2, 6, 12] suggesting that W-W interfacial decohesion does indeed initiate throughout these materials at an early stage of deformation. However the present authors [2] have determined that only approximately 3.3% of all W-W interfaces are cracked prior to rupture within this alloy during room temperature tensile tests. For temperatures up to and including room temperature this alloy has been shown to fracture without necking [17], the prime site of crack nucleation being the W-W interface with rupture proceeding by a cascade of nucleation events on all favourable sites leading to a fracture surface upon which all four of the possible fracture modes are fairly represented. The increased toughness of the W-binder interface with temperature together with the increased plasticity of the tungsten grains results in the samples failing within a necked region above the DBT temperature. Fracture within a neck takes place under a condition of triaxial stress with a higher tensile component, which together with the high plastic strains within the neck, allow crack linkages to be made through mechanisms of void growth and shear. If interfaces are sufficiently tough to enable load transfer and to allow large plastic strains, then there is every reason to expect that material failure will not be limited by the interfaces so that rupture is dominated by the bulk properties of the material, the tungsten phase.

Within these alloys we would expect to observe a correlation between the presence of W cleavage on the one hand and the absence of W-W interfacial decohesion on the other for the following reasons. As pointed out by Woodward and O'Donnell [2], for room temperature fracture, the fracture surface within these alloys tends to deviate by only one W grain diameter in or out of a nominal plane of fracture. With this in mind, all W grains in this plane will be represented in the fracture surface by either (i) a 'pocket' from where they have been pulled out, leaving behind the telltale W-W decohesion sites, (ii) a protruding W grain surface, which again reveals the W-W decohesion sites of its missing neighbours, or (iii) as a cleaved W grain. A decrease in W-W decohesion should therefore be balanced by an increase in W cleavage, since a grain which undergoes cleavage is 'hiding' the W-W decohesion sites which would otherwise be visible had it not cleaved. Fig. 3 however, indicates that the proportion of W-W decohesion only reduces slowly as the occurrence of W cleavage escalates.

Closer examination of the micrographs in Fig. 2 suggests that not all W-W interfaces are of the same size and fewer of the small interfaces are present in the higher temperature fracture surfaces. Therefore it is only those larger surface area W-W interfaces (the weakest links) which contribute to the fracture surface at high temperatures while those tungsten grains held more securely by the W-binder interface (i.e. having smaller W-W interfacial areas) are more likely to undergo cleavage fracture. Consequently, the total area of W-W decoherence reduces only slightly as W cleavage (with its larger contribution to the fracture surface area) substitutes for the smaller W-W decohesion contribution. Above 250°C, W cleavage begins to replace all the remaining W-W decohesion sites (with the possible exception of the small percentage of nuclei which exist throughout the body prior to necking [2]) causing a more rapid decrease in the total area contributed by W-W decohesion fracture.

It is clear that each of the four fracture mechanisms is of similar strength and the variation in the occurrence of each, as observed above, is, with the likely exception of W-W interfacial decohesion, closely related to the DBT temperature for this alloy and the relative temperature dependence of the flow stress of each phase. The lack of any abrupt variation in the plot of UTS v Temperature is consistent with this interpretation. The dependence of failure strain on temperature exhibited by this alloy, refer to Fig. 1, is also consistent with a composite whose major phase undergoes a broad ductile to brittle transition above about 0°C.

The variation of rupture mechanism with temperature in this alloy is therefore believed to derive from: (i) the size, orientation and spatial distribution of the weaker W-W interfaces, (ii) the stiffness and strength of the tungsten grains at lower temperatures resulting in a tungsten/binder strength differential which can lead to W-B interface rupture at such temperatures and (iii), a softening of the W phase relative to the binder phase at high temperatures allowing increased uniform plastic

strain and shifting towards a bulk fracture path, involving W grain cleavage as a more favourable mechanism. The shift between favoured mechanisms is emphasized by a change in the rupture process from a cascade of nucleation events at strains below necking in the low temperature tests to crack growth and linking within a necked region at the higher temperatures.

5. Conclusion

The 95 wt% W 3.5 wt% Ni 1.5 wt% Fe alloy investigated here undergoes a broad ductile to brittle transition above about 0°C. The appearance of tensile necking in samples deformed above this temperature and a maximum in tensile elongation above approximately 50°C is consistent with such a DBT temperature. Fracture within this material is through a combination of W-W intergranular decohesion, W-binder interfacial decohesion, binder rupture and W cleavage. The contributions of each of these fracture mechanisms to specimen rupture varies with deformation temperature. At high temperatures specimen rupture is almost exclusively through the W cleavage mechanism while at lower temperatures all mechanisms are well represented although W-binder decohesion is the most prevalent. The variation in fracture mode depends on the cohesion of the W-binder interface which experiences a shear stress which varies with temperature, and a softening of the tungsten grains which show increased plasticity at higher test temperatures. The differences with test temperature are highlighted by a change in rupture mode in the tensile test from nucleation dominated fracture without necking at low temperatures to fracture by void growth and coalescence within a necked region at higher temperatures.

Acknowledgements

The authors would like to acknowledge the valuable experimental and metallographic support for this work provided by Mr Steve Pattie, Mr Pat McCarthy and Mr Jim Dimas of DSTO.

References

1. E. C. GREEN, D. J. JONES and W. R. PITKIN, Iron Steel Inst. Spec. Rep. No. 58, 1954, p. 253. Symp. Powder Met.
2. R. L. WOODWARD and R. G. O'DONNELL, in "Tungsten and Tungsten Alloys," edited by A. Bose and R. Dowding (Metal Powder Industries Federation, Princeton, N.J., 1992) p. 389.
3. L. EKBOM, *Scandinavian Jnl of Met* **20** (1991) 190.
4. R. M. GERMAN, J. E. HANAFEE and S. L. DIGIALLONARDO, *Met. Trans.* **15A** (1984) 121.
5. W. E. GURWELL, Ann. Powder Metall. Conf. And Exhibition, Boston, MA, Metal Powder Industries Federation, May 1986, p. 1.
6. K. M. OSTALAZA ZAMORA, J. GIL SEVILLANO and M. FUENTES PEREZ, *Mat. Sci. Eng.* **A157** (1992) 151.
7. J. LANKFORD, A. BOSE and H. COUQUE, in "High Strain Rate Behaviour of Refractory Metals and Alloys," edited by R. Ashahani, E. Chen and A. Crowson (The Minerals, Metals and Materials Society, 1992) p. 267.
8. J. M. YELLUP, R. L. WOODWARD and M. E. DE MORTON, Materials Research Laboratory Technical Note MRL-TN-443, Dept of Defence, Commonwealth of Australia, October 1980.
9. E. G. ZUKAS and H. SHEINBERG, *Powder Technol.* **13** (1976) 85.
10. B. H. RABIN and R. M. GERMAN, *Met. Trans.* **19A** (1988) 1523.
11. M. R. EISENMANN and R. M. GERMAN, *Int. J. Refract Hard Met.* **3** (1984) 86.
12. R. G. O'DONNELL, S. J. ALKEMADE and R. L. WOODWARD, *J. Mat. Sci.* **27** (1992) 6490.
13. B. C. MUDDLE and D. V. EDMONDS, *Acta. Met.* **33** (1985) 2119.
14. J. B. POSTHILL, M. C. HOGWOOD and D. V. EDMONDS, *Powder Metall.* **29** (1986) 45.
15. R. M. GRMAN, L. L. BOURGUIGAN and B. H. RABIN, *J. Metals* **37** (1985) 36.
16. B. H. RABIN, A. BOSE and R. M. GERMAN, in "Microstructural Science, Vol 15," edited by M. E. Blum, P. M. French, R. M. Middleton and G. F. Vander Voort (Elsevier, New York, 1986) p. 285.
17. R. L. WOODWARD and R. G. O'DONNELL, *J. Mat. Sci.*, submitted.
18. R. G. O'DONNELL and R. L. WOODWARD, *Met. Trans.* **21A** (1990) 744.
19. R. L. WOODWARD, I. G. MCDONALD and A. GUNNER, *J. Mat. Sci. Letts* **5** (1986) 413.
20. R. L. WOODWARD, J. M. YELLUP and M. E. DE MORTON, *Met. Forum* **6** (1983) 175.

Received 6 August 1999
and accepted 14 February 2000